



Sudan University of Sciences and Technology

College of Graduate Studies

Estimation of Age by using MRI Brain

تقدير العمر باستخدام صور الرنين المغناطيسي للدماغ

**A Thesis Submitted in Partial Fulfillment for the
Requirements of Master Degree of Science in diagnostic
Radiological Technology**

Presented by:

Auis Bashir Mohamed

Supervised By:

Dr: Caroline Edward Ayad

February 2015

الآية:

قال تعالى:

(رَبِّ أَوْزِعْنِي أَنْ أَشْكُرَ نِعْمَتَكَ الَّتِي أَنْعَمْتَ عَلَيَّ وَعَلَى
وَالِدَيَّ وَأَنْ أَعْمَلَ صَالِحاً تَرْضَاهُ وَأَدْخِلْنِي بِرَحْمَتِكَ فِي
عِبَادِكَ الصَّالِحِينَ)

سورة النمل (19)

Acknowledgment

I wish to express my sincere thanks to Dr. Caroline Edward, for providing me with all the necessary facilities for this research.

And also I would like to thank everybody have a role in pushing me forward

Dedication

To whom I should give my all love to

To my soft-hearted mother

To my great father

To the soul of my best brother

(Loay)

To the humanity

Abstract:

This study is an attempt to estimate the human age by measuring the signal intensity of the brain gray and white matter on MRI T1weighted images.

The study was conducted at Garash international specialized hospital (Khartoum-Sudan) during the period from June up to October 2014.

Sixty consecutive subjects were selected in both gender and with different ages.

All subjects were scanned for axial brain using MRI 1.5 Tesla (Toshiba – vantage). T1 and T2 weighted images were obtained at areas including caudate nucleus head, thalamus, putamen, corpus callosum, forcipes minor and corona radiate. And the signal intensity was measured in T1weighted image and the data were correlated with age.

Results showed that there is significant negative relationship between the signal intensity of brain gray and white matter and subjects ages.

New equations were established to estimate the age for subjects with known brain signal intensity.

MRI T1 weighted image is suitable and recommended method for age estimation that because it is the best sequence to demonstrate the normal anatomy.

الخلاصة

تعتبر هذه الدراسة محاولة لتقدير عمر الانسان عن طريق قياس شدة الاشارة لطبقتي الدماغ الرمادية والبيضاء في صورة الرنين المغنطيسي في زمن الراحة الاول.

اجريت هذه الدراسة في مستشفى جرش الدولي التخصصي (الخرطوم – السودان) خلال الفترة من يونيو وحتى اكتوبر 2014.

تم اختيار عدد 60 عينة مختارة وفق مطلوبات الدراسة لكلا الجنسين وفي مختلف الاعمار.

كل العينات تم فحصها بواسطة الرنين المغنطيسي 1.5 تسلا (توشيا – فانتج) تم اجراء صور الرنين في زمن الراحة الاول والثاني.

تم اختيار اجزاء تشريحية محددة في الدماغ تشمل رأس النواة الذيلية , المهاد , البوتامين , الحاجز الأبيض , فورسبس ماينر والكورونا .

وتم قياس شدة الإشارة في صور الرنين المغنطيسي في زمن الراحة الأول وربط علاقتهم بالعمر .

أوضحت الدراسة وجود ارتباط معنوي بين شدة اشارة انسجة الدماغ والعمر

تم إنشاء معادلات للتنبؤ وتقدير العمر عن طريق قياس شدة الإشارة للدماغ .

تعتبر صور الرنين المغنطيسي في زمن الراحة الأول من الطرق المناسبة والموصى بها لتقدير العمر وذلك نسبة لانها افضل طريقة لاطهار التشريح الطبيعي للدماغ .

List of abbreviation:

AD Alzheimer disease

ADEM acute disseminated encephalomyelitis

ADH anti diuretic hormone

CNS central nervous system

CSF cerebrospinal fluid

CT computerized tomography

GH growth hormone

GM gray matter

MPR multi planer reconstruction

MRI magnetic resonance imaging

MS multiple sclerosis

NVD neurovascular disease

NVM net m vector machine

RH releasing hormone

RMV relevant magnetic vector

ROI region of interest

SI signal intensity

T1 T1wighted image

T2 T2wighted image

WM white matter

List of tables:

Table No	Title	Page
4.1	Subjects classification according to gender	32
4.2	Subjects classification according to age	33
4.3	Descriptive statistics of the variables GM and WM signal intensity(mean, min, and max values)	34
4.4	Correlation between the variables	35
4.5	Coefficient of variable (G1) with age	36
4.6	Coefficient of variable (G2) with age	37
4.7	Coefficient of variable (G3) with age	38
4.8	Coefficient of variable (W1) with age	39
4.9	Coefficient of variable (W2) with age	40
4.10	Coefficient of variable (W3) with age	41
4.11	Coefficient of variable (G1) with gender	42
4.12	Coefficient of variable (G2) with gender	42
4.13	Coefficient of variable (G3) with gender	42
4.14	Coefficient of variable (W1) with gender	43
4.15	Coefficient of variable (W2) with gender	43
4.16	Coefficient of variable (W3) with gender	43

List of figures

Figure No	Title	Page
2.1	Major parts of the brain	4
2.2	Brain lobes	5
2.3	Frontal lobe	7
2.4	Occipital lobe	9
2.5	Ventricular system	10
2.6	Cerebellar and brain stem	13
2.7	Structure of the neuron	16
4.1	Gender frequency and percentage	33
4.2	Age classes frequency and percentage	34
4.3	Scatter polite of the relationship between the age and signal intensity of the caudate nucleus head	36
4.4	Scatter polite of the relationship between the age and signal intensity of the thalamus	37
4.5	Scatter polite of the relationship between the age and signal intensity of the putamen	38
4.6	Scatter polite of the relationship between the age and signal intensity of the corpus callosum	39
4.7	Scatter polite of the relationship between the age and signal intensity of the forcipes minor	40
4.8	Scatter polite of the relationship between the age and signal intensity of the corona radiata	41

List of content	
الاية	I
Acknowledgment	Ii
Dedication	Iii
Abstract in English	Iv
Abstract in Arabic	V
List of abbreviations	Vi
List of tables	Vii
lest of figures	Viii
List of content	Ix
Chapter one	1
Introduction	
Prelude	1
Problem of the study	2
Objectives	3
Thesis scope	3
Chapter two literature review	4
Anatomy	4
Physiology	19
Pathology	20
Previous study	26
Chapter three Materials and Methods	30
Material	30

Methodology	30
Chapter four the results	32
Chapter five	
Discussion	44
Conclusion	45
Recommendations	46

Chapter one

Introduction

1.1 Prelude:

A determination of human age is important such as in the setting of a crime investigation because the age can guide investigators to the correct identity among a large number of possible matches. Traditional morphological methods used by anthropologists to determine age are often imprecise, whereas chemical analysis of tooth dentin, such as aspartic acid racemization, has shown reproducible and more precise results. (Kantar Alkass et al., 2009).

On this study we aimed to estimate the normal human age by measuring the MRI signal intensity of the brain gray/white matter using MRI scanner. The idea of this study had come out from much previous studies result in that there are significant histological changes occur to the human brain due to normal aging beside the pathological changes. These changes appear in the MRI signal intensity that we use to perform this study.

Magnetic resonance imaging (MRI) is a non- invasive imaging tool that utilizes a strong magnetic field and radio frequency waves to visualize in great detail organs. Unlike conventional x-rays (including computed tomography, there is no exposure to ionizing radiation and at most field strengths (generally below 7 Tesla) the procedure is considered safe for nearly every age group. Because it is non-invasive (i.e., does not break the skin or harm the body) and possesses excellent spatial resolution, the use of MRI as a research tool has increased exponentially over the past decade. Uses have ranged from add-ons to a clinical study (Gilmore JH, et al 2006.) Magnetic resonance (MR) is based upon the

interaction between an applied magnetic field and a nucleus that possesses spin. Nuclear spin or, more precisely, nuclear spin angular momentum, is one of several intrinsic properties of an atom and its value depends on the precise atomic composition. (Mark and Richard 2003,)

1.2 MRI signal intensity:

As a result of resonance, the NMV is precessing in phase in the transverse plane. Faraday's law of induction states that if a receiver coil or any conductive loop is placed in the area of a moving magnetic field, i.e. the NMV precessing in the transverse plane, a voltage is induced in this receiver coil. A signal is produced when coherent (in phase) magnetization cuts across the coil. As the NMV precesses at the Larmor frequency in the transverse plane, a voltage is induced in the coil. This voltage constitutes the MRI signal. The frequency of the signal is the same as the Larmor frequency – the magnitude of the signal depends on the amount of magnetization present in the transverse plane, which depends upon the characteristics of the tissue under examination. (Catherine and Carolyn 2000)

1.3 Problem of the study:

Characteristics of the brain, gray and white matter are different from body to body. This difference may be due to normal aging, development or pathological conditions.

1.4 Objectives:

1.4.1 General objective:

Estimation of human age by measuring the MRI signal intensity of the gray and white matter of the brain in the normal subjects

1.4.2 Specific objectives:

Characterize the gray matter and white matter by measuring their MRI signal intensities

To evaluate the signal intensity of the gray matter and white matter

To correlate the finding with the subjects chronological age and gender

To compare the chronological age with the estimated age

1.5 Thesis scope

Chapter one included the introduction, problem of the study and objective, chapter two concerned with literature review, chapter three dealt with the methods and materials that used on this study, chapter four showed the result of the study. Chapter five discussed the result of the study

Chapter two

Literature review

Anatomy, physiology and pathology

2.1 anatomy of the brain

The brain consists of many parts that function as an integrated whole. The major parts are the cerebrum, the cerebellum, brain stem (medulla, pons, midbrain) the hypothalamus, the thalamus and the ventricular system. All these parts are interconnected and work together (*Valerie C. Scanlon 2007*).

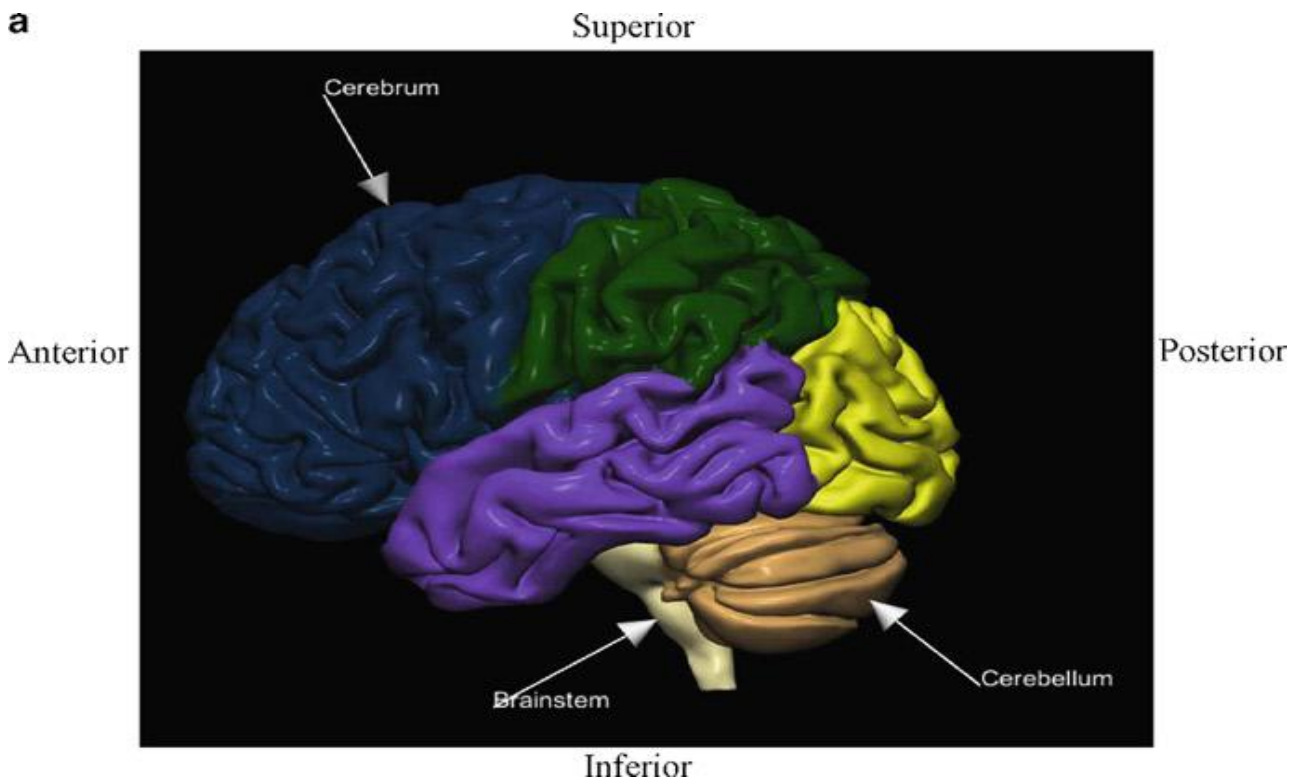


Fig (2.1) shows the major parts of the brain (Wieslaw L. Nowinski 2011)

2.1.1 Cerebrum

The largest part of the human brain is the cerebrum, which consists of two hemispheres separated by the longitudinal fissure. At the base of this deep groove is the corpus callosum, a band of 200 million neurons that connects the right and left hemispheres. Within each hemisphere is a lateral ventricle.

The surface of the cerebrum is gray matter called the cerebral cortex. Gray matter consists of cell bodies of neurons, which carry out the many functions of the cerebrum. Internal to the gray matter is white matter, made of myelinated axons and dendrites that connect the lobes of the cerebrum to one another and to all other parts of the brain in the human brain the cerebral cortex is folded extensively. The folds are called convolutions or gyri and the grooves between them are fissures or sulci this folding permits the presence of millions more neurons in the cerebral cortex. The cerebral cortex is divided into lobes that have the same names as the cranial bones external to them. Therefore, each hemisphere has a frontal lobe, parietal lobe, temporal lobe, and occipital lobe. .
(Valerie C. Scanlon 2007)

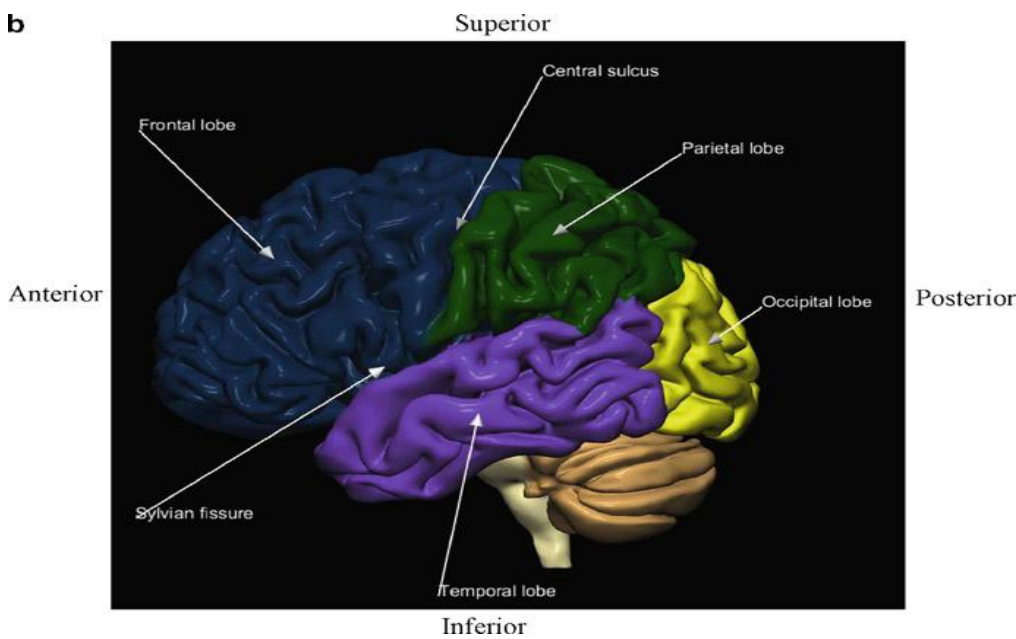


Fig (2.2) shows the brain lobes (Wieslaw L. Nowinski 2011)

2.1.1.1 Frontal lobes

On its lateral aspect, the frontal lobe extends from the frontal pole to the central sulcus, constituting the anterior one-third of the cerebral cortex. Its posteriormost gyrus, the precentral gyrus, consists of the primary motor area and is bordered anteriorly by the precentral sulcus and posteriorly by the central sulcus. The region of the frontal lobe located anterior to the precentral sulcus is subdivided into the superior, middle, and inferior frontal gyri. This subdivision is due to the presence, though inconsistent, of two longitudinally disposed sulci, the superior and inferior frontal sulci. The inferior frontal gyrus is demarcated by extensions of the lateral fissure into three subregions: the pars triangularis, pars opercularis, and pars orbitalis. In the dominant hemisphere, a region of the inferior frontal gyrus is known as Broca's area, which functions in the production of speech. On its inferior aspect, the frontal lobe presents the longitudinally disposed olfactory sulcus. Medial to this sulcus is the gyrus rectus (also known as the straight gyrus), and lateral to it are the orbital gyri. The olfactory sulcus is partly occupied by the olfactory bulb and olfactory tract its posterior extent, the olfactory tract bifurcates to form the lateral and medial olfactory striae. The intervening area between the two striae is triangular in shape and is known as the olfactory trigone and it abuts the anterior perforated substance. On its medial aspect, the frontal lobe is bordered by the arched cingulate sulcus, which forms the boundary of the superior aspect of the cingulate gyrus. The quadrangular-shaped cortical tissue anterior to the central sulcus is a continuation of the precentral gyrus and is known as the anterior paracentral lobule (Maria and Leslie 2006)

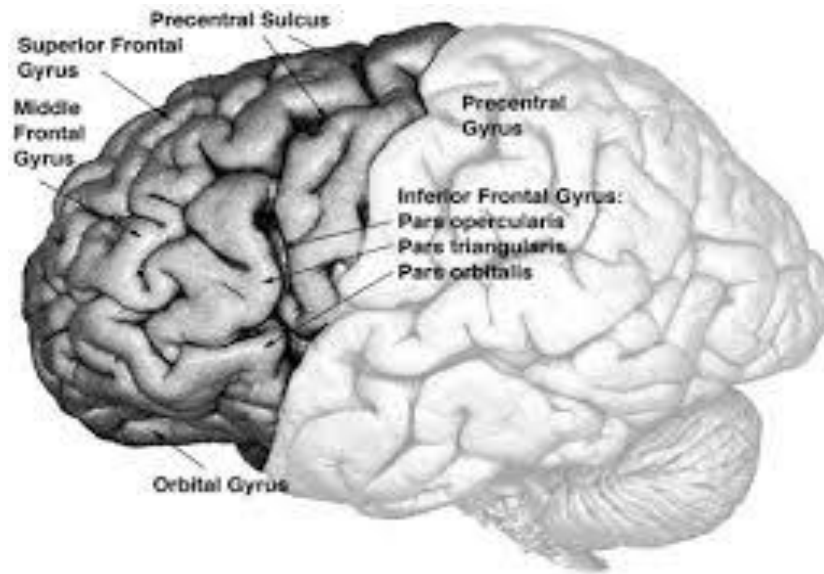


Fig (2.3) anatomy of the frontal lobe

2.1.1.2 Parietal Lobes

The parietal lobe is interposed between the frontal and occipital lobes and is situated above the temporal lobe. On its lateral aspect, its anterior most gyrus, the post central gyrus, is the primary somesthetic area to which primary somatosensory information is channeled from the contra lateral half of the body. The remainder of the parietal lobe, separated from the post central gyrus by the post central sulcus, is subdivided by the inconsistent intraparietal sulcus, into the superior and inferior parietal lobules. The former is an association area involved in somatosensory function, whereas the latter is separated into the supramarginal gyrus, which integrates auditory, visual, and somatosensory information, and the angular gyrus on its medial aspect, the parietal lobe is separated from the occipital lobe by the parieto-occipital sulcus and its inferior continuation, the calcarine fissure. This region of the parietal lobe is subdivided into two major

structures, the inferiorly positioned posterior parietal lobule and the posteriorly situated precuneus.

2.1.1.3 Temporal Lobe:

The temporal lobe is separated from the frontal and parietal lobes by the lateral fissure and from the occipital lobe by an imaginary plane that passes through the parieto-occipital sulcus. The anteriormost aspect of the temporal lobe is known as the temporal pole. On its lateral aspect, the temporal lobe exhibits three parallel gyri, the superior, middle, and inferior temporal gyri, separated from each other by the inconsistently present superior and middle temporal sulci. The superior temporal gyrus of the dominant hemisphere contains Wernicke's area. The inferior aspect of the temporal lobe is grooved by the inferior temporal sulcus that is interposed between the inferior temporal gyrus and the lateral occipitotemporal gyrus (fusiform gyrus). The collateral sulcus separates the fusiform gyrus from the parahippocampal gyrus of the limbic lobe (Maria and Leslie 2006)

2.1.1.4 Occipital Lobe:

The occipital lobe extends from the occipital pole to the parieto-occipital sulcus. On its lateral aspect, the occipital lobe presents the superior and inferior occipital gyri, separated from each other by the horizontally running lateral occipital sulcus. On its medial aspect, the occipital lobe is subdivided into the superiorly located cuneate gyrus (cuneus) and the inferiorly positioned lingual gyrus, separated from each other by the calcarine fissure. The cortical tissue on each bank of this fissure is known collectively as the striate cortex (calcarine cortex), and forms the primary visual cortex

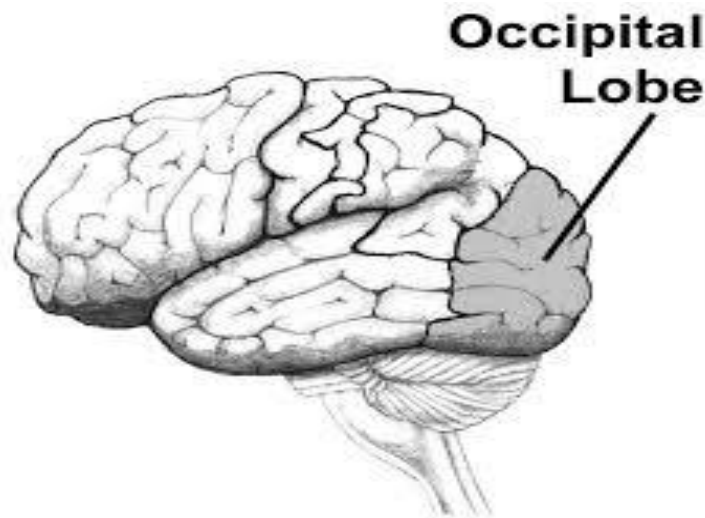


Fig (2.4) demonstrate the occipital lobe

2.1.1.5 Limbic lobe:

The limbic lobe is a complex region and includes the cingulate gyrus, parahippocampal gyrus, hippocampal formation, subcallosal gyrus, parolfactory gyrus, and the preterminal gyrus. The following description is a view of the medial aspect of the hemisected brain and the various regions of the corpus callosum are obvious landmarks. Therefore, the corpus callosum will now be described, even though it is not a part of the limbic lobe. The anterior extent of the corpus callosum, known as the genu, bends inferiorly and turns posteriorly, where it forms a slender connection, the rostrum, with the anterior commissure. The posterior extent of the corpus callosum is bulbous in shape, and is known as the splenium the cingulate gyrus is located above the corpus callosum and is separated from it by the callosal sulcus. As the cingulate gyrus continues posteriorly, it follows the curvature

of the corpus callosum and dips beneath the splenium to continue anteriorly as the isthmus of the cingulate gyrus. The anterior continuation of the isthmus is the parahippocampal gyrus whose anteriormost extent is known as the uncus.

Above the parahippocampal gyrus is the hippocampal sulcus, which separates the parahippocampal gyrus from the hippocampal formation (composed of the hippocampus, subiculum, and dentate gyrus). Just beneath the rostrum of the corpus callosum is the subcallosal gyrus. The connection between the anterior commissure and the optic chiasma is the lamina terminalis and the cortical tissue anterior to the lamina terminalis is the parolfactory gyrus and preterminal gyrus. The subcallosal, parolfactory, and preterminal gyri are referred to as the subcallosal area (Maria and Leslie 2006).

2.1.2 Ventricles

The ventricles are four cavities within the brain: two lateral ventricles, the third ventricle, and the fourth ventricle each ventricle contains a capillary network called a choroid plexus, which forms cerebrospinal fluid (CSF) from blood plasma. Cerebrospinal fluid is the tissue fluid of the central nervous system.

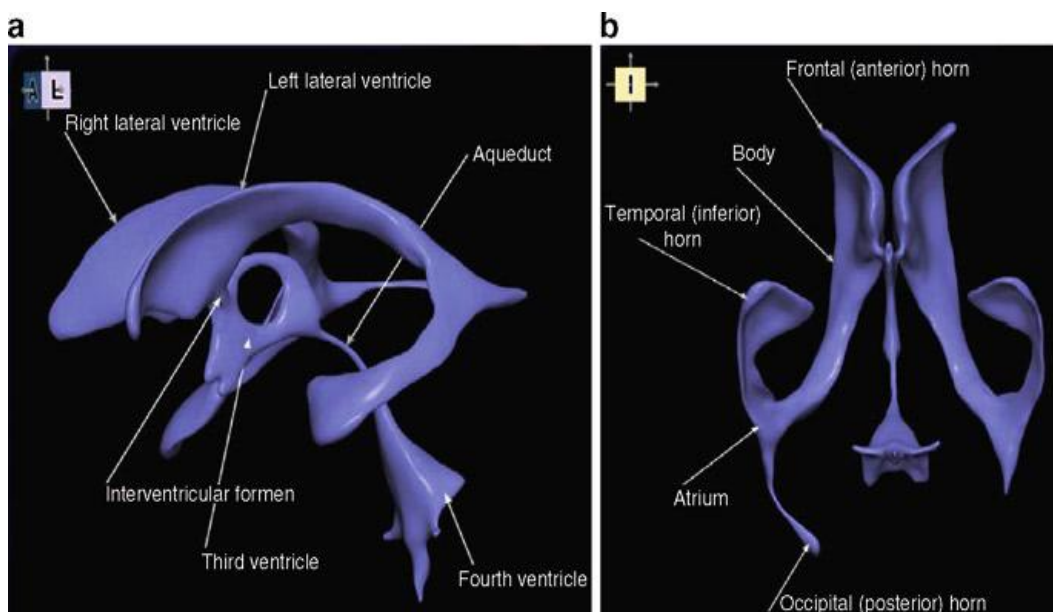


Fig (2.5) shows the ventricular system (Wieslaw L. Nowinski 2011)

2.2 Cerebellum

The cerebellum is located in the posterior aspect of the brain, just below the occipital lobes of the cerebrum. It is separated from the cerebrum via a horizontal dural reflection, the tentorium cerebelli. The cerebellum is connected to the midbrain, pons, and medulla of the brainstem via three pairs of fiber bundles, the superior, middle, and inferior cerebellar peduncles, respectively. Viewing the cerebellum, it can be seen that it is composed of the right and left cerebellar hemispheres and the narrow, intervening vermis. The vermis is also subdivided into a superior and an inferior portion, where the superior portion is visible between the two hemispheres, while its inferior portion is buried between the two hemispheres. The surface of the cerebellum has horizontal elevations, known as folia, and indentations between the folia, known as sulci. Some of these sulci are deeper than others and they are said to subdivide each hemisphere into three lobes, the small anterior lobe, the much larger posterior lobe, and the inferiorly positioned flocculonodular lobe (formed from the nodule of the vermis and the flocculus of each cerebellar hemisphere). The anterior lobe is separated from the posterior lobe by the primary fissure, and the posterolateral fissure separates the flocculonodular lobe from the posterior lobe. Similar to the cerebrum, the cerebellum has an outer rim of gray matter, the cortex, an inner core of nerve fibers, the medullary white matter, and the deep cerebellar nuclei, located within the white matter. The cortex and white matter are easily distinguished from each other in a midsagittal section of the cerebellum, where the white matter arborizes, forming the core of what appears to be a tree-like architecture, known as the arbor vitae. Histologically, the cerebellar cortex is a three-layered structure, the outermost molecular layer, the middle Purkinje layer, and the innermost granular layer. The granular layer is well defined due to the presence of nucleic acids in the nuclei of its numerous, small cells. The Purkinje

layer, composed of a single layer of large Purkinje cell perikaryons, is also easily recognizable. The molecular layer is rich in axons and dendrites as well as capillaries that penetrate deep into this layer. Four pairs of nuclei are located within the substance of the cerebellar white matter. These are the fastigial, dentate, emboliform, and globose nuclei. The connections between the cortical regions and the deep nuclei of the cerebellum permit the subdivision of the cerebellum into three zones—the vermal, paravermal, and hemispheric—where each zone is composed of deep cerebellar nuclei, white matter, and cortex. (Maria and Leslie 2006)

2.3 The brain stem:

The brain stem is composed of medulla, pons and midbrain

2.3.1 Medulla:

The medulla extends from the spinal cord to the pons and is anterior to the cerebellum.

2.3.2 Pons:

The Pons bulges anteriorly from the upper part of the medulla. Within the pons are two respiratory centers that work with those in the medulla to produce a normal breathing rhythm.

The many other neurons in the pons (pons is from the Latin for “bridge”) connect the medulla with other parts of the brain.

2.3.3 Mid brain:

The midbrain extends from the pons to the hypothalamus and encloses the cerebral aqueduct, a tunnel that connects the third and fourth ventricles..

(Valerie C. Scanlon 2007)

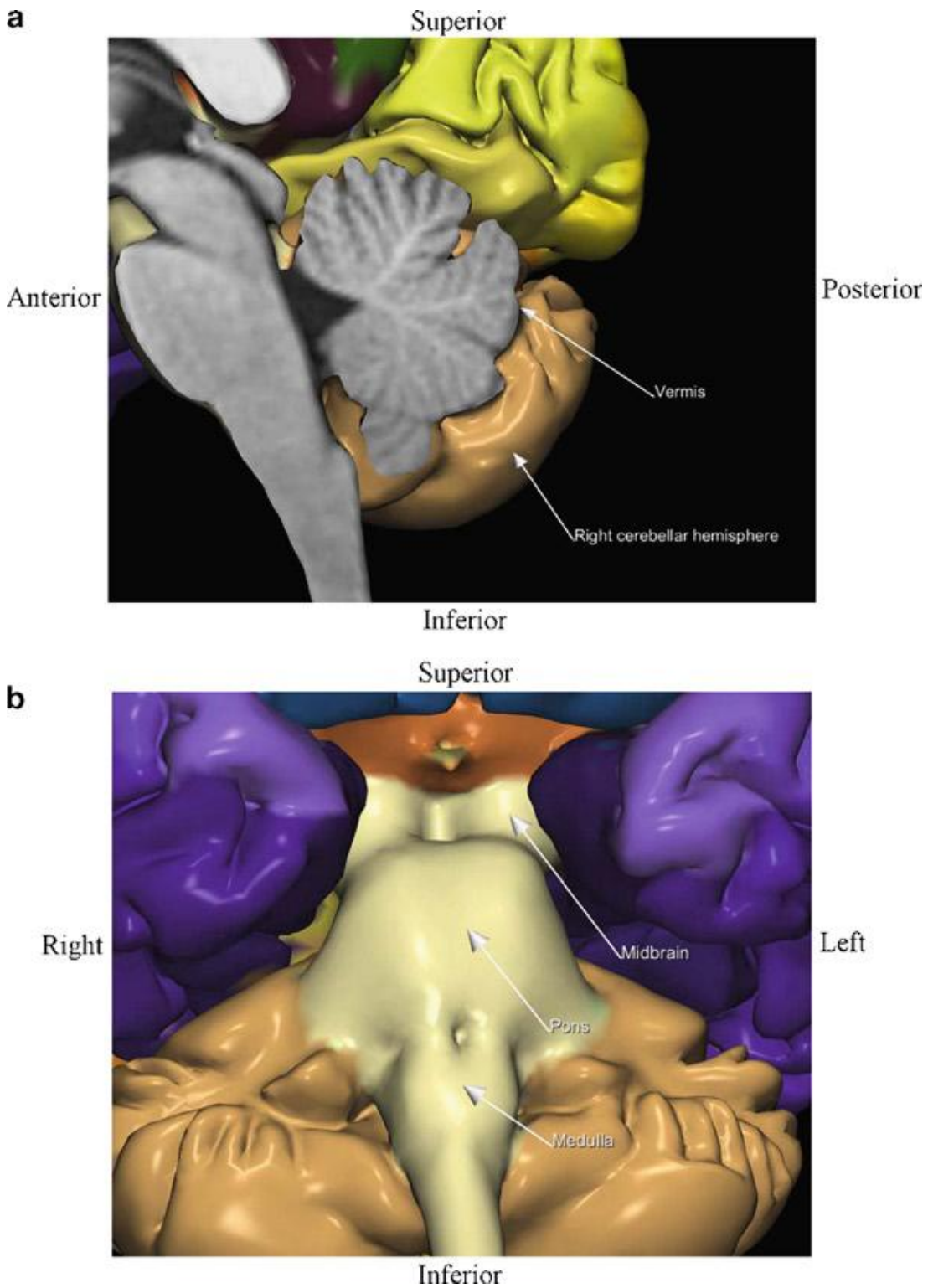


Fig (2.6) cerebellum and brain stem (Wieslaw L. Nowinski 2011)

2.4 Hypothalamus

Located superior to the pituitary gland and inferior to the thalamus, the hypothalamus is a small area of the brain with many diverse functions

2.5 Thalamus

The thalamus is superior to the hypothalamus and inferior to the cerebrum. The third ventricle is a narrow cavity that passes through both the thalamus and hypothalamus.

2.6 Basal Ganglia

The basal ganglia, called ganglia even though they are nuclei, are large collections of cell bodies that are embedded deep in the white matter of the brain. These soma include those deep nuclei of the brain and brainstem which, when damaged, produce movement disorders. Thus the basal ganglia are composed of the caudate nucleus, lenticular nucleus (putamen and globus pallidus), subthalamic nucleus of the ventral thalamus, and the substantia nigra of the mesencephalon (the caudate nucleus and the putamen together are referred to as the striatum). These nuclei have numerous connections with various regions of the CNS; some receive input and are categorized as input nuclei, some project to other regions and are referred to as output nuclei, whereas some receive input, project to other regions of the CNS, and have local interconnections and these are known as intrinsic nuclei

(Maria and Leslie 2006)

2.7 Micro anatomy of the brain

2.7.1 Neuron:

Nerve cells are called neurons, or nerve fibers. Whatever their specific functions, all neurons have the same physical parts. The cell body contains the nucleus and is essential for the continued life of the neuron. Neuron cell bodies are found in the central nervous system (**fig 2.7**) or close to it in the trunk of the body. In these locations, cell bodies are protected by bone. There are no cell bodies in the arms and legs, which are much more subject to injury. Dendrites are processes (extensions) that transmit impulses toward the cell body. The one axon of a neuron transmits impulses away from the cell body. It is the cell membrane of the dendrites, cell body, and axon that carries the electrical nerve impulse. In the peripheral nervous system, axons and dendrites are “wrapped” in specialized cells called Schwann cells (see Fig. 2–1). During embryonic development, Schwann cells grow to surround the neuron processes, enclosing them in several layers of Schwann cell membrane. These layers are the myelin sheath

2.7.2 Myelin:

Is a phospholipid that electrically insulates neurons from one another. Without the myelin sheath, neurons would short-circuit; just as electrical wires would if they were not insulated. The spaces between adjacent Schwann cells, or segments of the myelin sheath, are called nodes of Ranvier (neurofibril nodes). These nodes are the parts of the neuron cell membrane that depolarize when an electrical impulse is transmitted. The nuclei and cytoplasm of the Schwann cells are wrapped around the outside of the myelin sheath and are called the neurolemma, which becomes very important if nerves are damaged. If a peripheral nerve is severed and reattached precisely by microsurgery, the axons and dendrites may regenerate through the tunnels formed by the neurolemmas.

In the central nervous system, the myelin sheaths are formed by oligodendrocytes, one of the neuroglia (glial cells), the specialized cells found only in the brain and spinal cord. Yet another type of glial cell is the astrocyte. In the embryo, these cells provide a framework for the migrating neurons that will form the brain. Thereafter, the extensions of astrocytes are wrapped around brain capillaries and contribute to the blood–brain barrier, which prevents potentially harmful waste products in the blood from diffusing out into brain tissue.

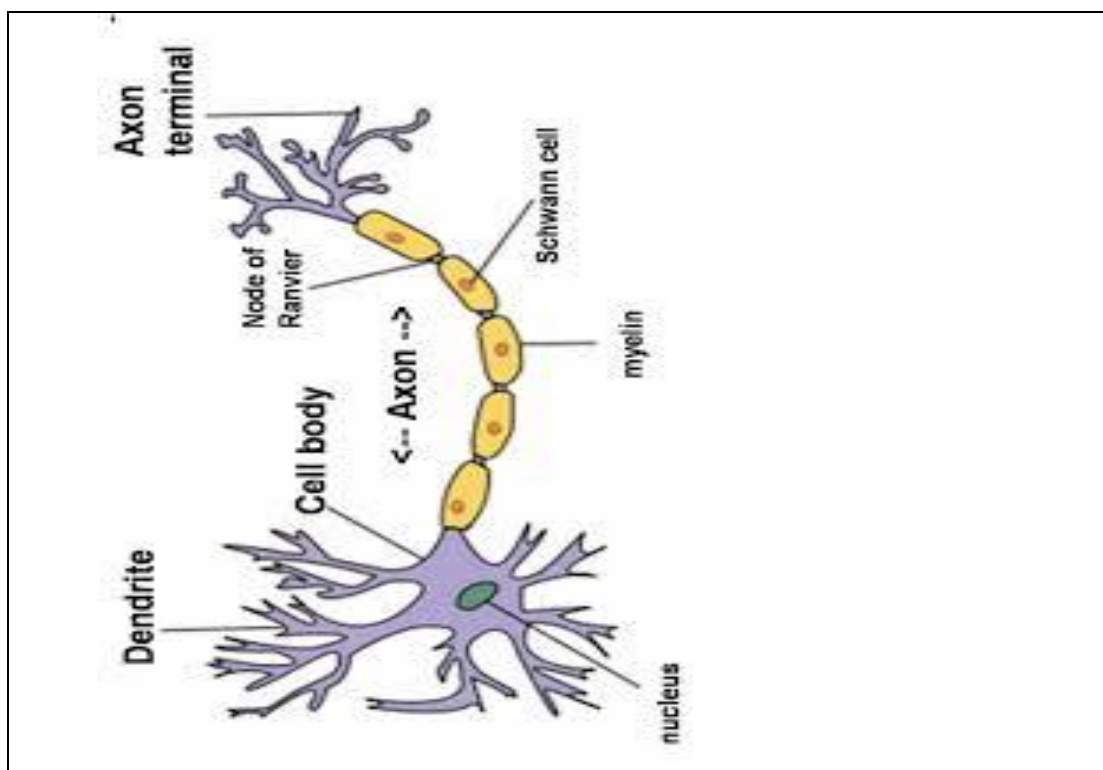


Figure (2.7). Neuron structure (Wieslaw L. Nowinski 2011).

2.7.3 Synapses

The small gap or space between the axon of one neuron and the dendrites or cell body of the next neuron is called the synapse. Within the synaptic knob of the presynaptic axon is a chemical neurotransmitter that is released into the synapse

by the arrival of an electrical nerve impulse The neurotransmitter diffuses across the synapse, combines with specific receptor sites on the cell membrane of the postsynaptic neuron, and there generates an electrical impulse that is, in turn, carried by this neuron's axon to the next synapse, and so forth. A chemical inactivator at the cell body or dendrite of the postsynaptic neuron quickly inactivates the neurotransmitter.

2.7.4 Types of Neurons:

Neurons may be classified into three groups: sensory neurons, motor neurons, and interneurons. Sensory neurons (or afferent neurons) carry impulses from receptors to the central nervous system. Motor neurons (or efferent neurons) carry impulses from the central nervous system to effectors. Sensory and motor neurons make up the peripheral nervous system. Visceral motor neurons form the autonomic nervous system, Interneurons are found entirely within the central nervous system. They are arranged so as to carry only sensory or motor impulses

2.7.5 Micro structure of the cerebrum and cerebellum:

2.7.5.1 Cerebrum:

Cortex gray matter; layered (4 - 6 layers, not as distinct as layers of the cerebellum) Molecular or plexiform layer (outer layer of gray matter) The molecular layer consists of dendrites and axons of neurons from underlying layers, scattered cell bodies of horizontal neurons and gray matter neuroglia.

Outer or external granular layer is small pyramidal neuron and stellate, granule neuron cell bodies and gray matter neuroglia, outer or external pyramidal layer larger is pyramidal neuron and small granule neuron cell bodies and gray matter neuroglia, Inner or internal granular layer is small stellate granule neuron cell bodies and gray matter neuroglia, Inner or internal pyramidal layer (ganglionic layer) medium to large pyramidal neuron cell bodies and smaller stellate neuron

cell bodies and gray matter neuroglia, Polymorphic layer (inner gray matter layer) next to the medulla. Neuron cell bodies of varying shapes (pyramidal, stellate, fusiform) and gray matter neuroglia, medullary core or medulla of the cerebrum white matter Axons entering and leaving the cortex and white matter neuroglia comprise the medulla of the cerebrum. This layer is typical white matter tissue.

2.7.5.2 Cerebellum

Cortex = gray matter arranged in three layers:

Outer layer = molecular layer, the molecular layer contains fewer cell bodies than the deeper layers of the cortex. Cell bodies visible in the molecular layer include stellate and basket neurons (multipolar neurons) and gray matter neuroglia (protoplasmic astrocytes, oligodendrocytes, microglia). Dendrites of the Purkinje neurons are a major component of the neuropil in the molecular layer. Middle layer (Purkinje cell layer), the Purkinje cell layer is characterized by large neuron cell bodies (Purkinje cells) with extensive dendritic "trees". Purkinje neuron dendrites extend into the outer molecular layer and their axons run down through the granular layer of the cortex into the white matter of the medulla. Inner layer (granular layer), the granular layer contains many cell bodies. These include small granule neurons, large stellate neurons, and gray matter neuroglia (protoplasmic astrocytes, oligodendrocytes, and microglia). The granular layer also contains axons of the Purkinje neurons.

Medullary core or medulla of the cerebellum is a white matter Axons entering and leaving the cortex and white matter neuroglia comprise the medulla of the cerebellum.

2.2 Physiology of the brain

The brain is found in the cranial cavity. Within it are found the higher nerve centers responsible for coordinating the sensory and motor systems of the body. The brain stem houses the lower nerve centers (consisting of midbrain, pons, and medulla),

2.2.1 Cerebrum:

The cerebrum, or top portion of the brain, is divided by a deep crevice, called the longitudinal sulcus. The longitudinal sulcus separates the cerebrum into the right and left hemispheres. In the hemispheres you will find the cerebral cortex, basal ganglia and the limbic system. The two hemispheres are connected by a bundle of nerve fibers called the corpus callosum. The right hemisphere is responsible for the left side of the body while the opposite is true of the left hemisphere. Each of the two hemispheres are divided into four separated lobes: the frontal in control of specialized motor control, learning, planning and speech; parietal in control of somatic sensory functions; occipital in control of vision; and temporal lobes which consists of hearing centers and some speech. Located deep to the temporal lobe of the cerebrum is the insula. (Wiki books contributors 2007)

2.2.2 Cerebellum:

The cerebellum is the part of the brain that is located posterior to the medulla oblongata and pons. It coordinates skeletal muscles to produce smooth, graceful motions. The cerebellum receives information from our eyes, ears, muscles, and joints about what position our body is currently in. It also receives output from the cerebral cortex about where these parts should be. After processing this information, the cerebellum sends motor impulses from the brainstem to the skeletal muscles. The main function of the cerebellum is coordination. The

cerebellum is also responsible for balance and posture. It also assists us when we are learning a new motor skill, such as playing a sport or musical instrument.

2.2.3 Medulla:

The medulla is the control center for respiratory, cardiovascular and digestive functions.

2.2.4 Pons:

The pons houses the control centers for respiration and inhibitory functions. Here it will interact with the cerebellum.

2.2.5 The Limbic System

The Limbic System is a complex set of structures found just beneath the cerebrum and on both sides of the thalamus. It combines higher mental functions, and primitive emotion, into one system. It is often referred to as the emotional nervous system. It is not only responsible for our emotional lives, but also our higher mental functions, such as learning and formation of memories. The Limbic system explains why some things seem so pleasurable to us, such as eating and why some medical conditions are caused by mental stress, such as high blood pressure. There are two significant structures within the limbic system and several smaller structures that are important as well. They are: The Hippocampus, amygdala, thalamus, hypothalamus, fornix and Para hippocampus, and the cingulate Gyrus (wikibooks contributors 2007)

2.3 Brain pathology

2.3.1 Neurodegenerative disorders:

Neurodegenerative disorders must be distinguished from normal aging. The neurodegenerative disorders are characterized by loss of functionally related groups of neurons anatomically. Clinical manifestations reflect the functional

loss which can be correlated anatomically in many situations. The following is a brief correlation of symptoms to lots of specific neuronal populations:

Cortical neurons: dementia, basal ganglia neurons, cerebellar neurons and motor neurons: Weakness. The etiology is not clear but current attention has been paid to chronic cellular injury, neurotoxin, stress at the cellular level, and cellular injury from excitotoxicity, damage due to free radicals. Some of the neurodegenerative are genetically transmitted. Expansion of trinucleotide repeats in the gene involved is identified in these disorders

Three major function of the CNS cognition and affect, motor, autonomic function. Clinically, neurodegenerative diseases usually manifest as disturbance of one of these three functions or in combinations as their chief manifestation. Examples are as follows:

Alzheimer's disease, frontotemporal dementia: language skill and frontal lobe symptoms, Parkinson's disease, amyotrophic lateral sclerosis, diffuse Lewy body disease: Motor and cognition and multiple system atrophy: Autonomic dysfunction (including orthostatic hypotension, impotence) and other dysfunctions such as Parkinsonism. (Kar-Ming Fung 2006)

2.3.2 Demyelinating disease:

Incidence: Demyelinating diseases, particularly multiple sclerosis, are common. Demyelination is loss of normal myelin that has already been formed. And dysmyelination is Failure to form normal myelin or maintain normal myelination as in leuko dystrophies.

Classifications:

Primary Demyelinating diseases:

Multiple sclerosis and inflammatory demyelinating pseudotumor

Secondary Demyelinating diseases:

Central pontine myelinolysis and Acute disseminated perivenous encephalomyelitis (acute perivascular myelinoclasia), Classic (parainfectious postimmunization idiopathic), Hyperacute (acute hemorrhagic leukoencephalitis) and Progressive multifocal leukodystrophy.

Multiple Sclerosis (MS):

Characteristic: A chronic, often relapsing, demyelinating disease with onset most commonly seen in young adults. The mean age of onset is 30 year-old; unusual to have onset in children under 10 year-old. More common in females, male to female ratio is 1:2 in adults, 1:10 in children.

Clinical features:

Chronic relapsing disease. About 10% of the patients continue to progress without remission. Optic neuritis and double vision are very often. Severity of clinical manifestation may not reflect the extent of pathologic change.

Neuroimaging:

MRI is the most sensitive method of detection. Periventricular white matter adjacent to the body and the trigones of the lateral ventricle. The plaques are often ovoid and with long axis parallel to the ventricles Enhancement is seen in acute plaques but not chronic plaque.

Gross pathology:

Plaque: Almond to oval lesions that range from a few mm to a few cm. Periventricular, optic nerve, spinal cord as most common locations. Affect predominantly the white matter.

Histology:

Affect predominantly the white matter. Often with multiple lesions at different stages of evolution. Perivascular chronic inflammation with loss of myelin. Three stages: acute, subacute, chronic (burnt out) plaque. Reactive gliosis are

more prominent in chronic plaques, inflammation is more prominent in acute plaques.

Variants of Multiple Sclerosis (MS)

Classic type: Charcot type.

Relapsing disease in many patients. Some patients may have only one episode. Some patients may not have remission but continuous progression.

Marburg type: Acute multiple sclerosis. This is a highly malignant form that progresses to death in a few weeks to a few months without remission in many cases.

Concentric sclerosis: Characteristic concentric rings of demyelination and partial remyelination. May be more common in Asian. Clinically similar to Marburg type and progresses to death rapidly.

Diffuse sclerosis: Often seen in children; also seen in adults. Large demyelinating lesions. Often progresses to death in 1-2 years.

Neuromyelitis optica:

Acute or subacute onset of blindness in one or both eyes preceded or followed within days or weeks by a transverse or ascending myelitis. The course is frequently rapidly progressive. May be more common in Asians.

Acute Disseminated Encephalomyelitis: Characterized by an acute multifocal inflammatory and demyelinating disease that is often associated with a preceding infectious illness. The clinical features are generally no fever and normal peripheral white count if the primary infection has subsided, CSF with lymphocytic pleocytosis, acute onset of somnolence, confusion, and often convulsion. May progress to coma in severe cases. Symptoms and signs often resolve over several weeks and relapses are very rare. Mortality 20% during acute illness. Permanent neurologic deficits in some patients.

Gross Pathology:

Swelling and edema; the brain is otherwise free of macroscopic pathologic changes.

Histology:

Multifocal perivenous lymphocytic infiltration. Inflammatory cells extend into surrounding parenchyma. Demyelination with the blood vessels as the epicenters.

Acute Hemorrhagic Leukoencephalopathy

Characterized by The most fulminant form of demyelinating disease and the patients usually die within days. The affected age mainly young adults, sometimes children. Clinical features are similar to ADEM but far more severe. Leukocytosis sometimes reaching 30,000 cells/mm³. Elevated erythrocyte sedimentation rate. CSF with polymorphonuclear leukocytosis, up to 3000 cells/mm³.

Gross Pathology:

The brain is swollen and soft, predominantly small but occasionally large hemorrhagic foci involving mostly the cerebrum and cerebellum and white matter in the pons.

Histology:

Mixed acute and chronic inflammatory cell infiltration. Rings and balls of hemorrhage: Blood vessels with fibrinoid necrosis rimmed by necrotic tissue and a larger zone of hemorrhage. Perivascular demyelination.

Central Pontine Myelinolysis

Characteristic: A non-inflammatory, acute, demyelinating disease that typically affects the pons and often associated with hyponatremia in alcoholics.

Gross Pathology: Affects the upper pons. Typically a butterfly or triangular shaped symmetrical midline lesion rimmed by areas with preserved myelination.

Histology:

No inflammation, macrophages are present, preserved axons; axonal swelling may be present, viable neurons in affected areas, transverse (pontocerebellar) fibers are more affected than the rostral-caudal (cortical spinal and cortical bulbar) fibers. (Kar-Ming Fung 2006)

2.3.3 Infection:

Just like any other organs in the human body, the central nervous system can be infected by all kinds of infectious agents including prion, virus, bacteria, fungus, and parasites. Similar to other organs of the body, infection of the CNS triggers inflammation in most cases. There are, however, some unique features regarding infections of the CNS:

Encephalitis without identified infectious agents.

This is a class of diseases featured by inflammation of the CNS that closely suggest infections but the infectious agents have never been isolated. Raussmussen encephalitis is a good example. Infections of the central nervous system come in 4 major patterns; diffuse, localized, multifocal and disseminated (infection form a primary source outside the CNS). There are important factors take parts in casting the final pathologic features: Virulence of the agent, Route of entry and Systemic factors such as compromised immunity.

Infections of the CNS can be classified into the following categories:

Meningitis, meningoencephalitis encephalitis, Myelitis, Encephalomyelitis Choroid plexitis, subdural empyema and epidural abscess, cerebritis Ventriculitis and ependymitis and brain abscess

Routes of entry:

Remote: Blood borne pathogen, abscess and source of infection in other part of the body.

Local: Paranasal sinuses and middle ear, olfactory epithelium, infection in adjacent soft tissue and bone, penetrating trauma, contaminated surgical procedures and/or hardware such as ventricular-peritoneal shunt.

Systemic factors:

Acquired and congenital immunodeficiency

Radiation therapy and chemotherapy

Diabetes, malnutrition

Steroid therapy

Ogan transplantation and bone marrow transplantation

Others. (Kar-Ming Fung 2006)

2.4 the previous study:

Franke K et al; 2007 studied Model of healthy brain aging. To Estimate the age of healthy subjects from T1-weighted MRI There, they introduce a framework for automatically and efficiently estimating the age using a kernel method for regression. This method was tested on over 650 healthy subjects, aged 19-86 years, and collected from four different scanners. Furthermore, the influence of various parameters on estimation accuracy was analyzed. Their age estimation framework included automatic preprocessing of the T1-weighted images, dimension reduction via principal component analysis, training of a relevance vector machine (RVM; Tipping, 2000) for regression, and finally estimating the age of the subjects from the test samples. The framework proved to be a reliable, scanner-independent, and efficient method for age estimation in healthy subjects, yielding a correlation of $r=0.92$ between the estimated and the real age

in the test samples and a mean absolute error of 5 years. The results indicated favorable performance of the RVM and identified the number of training samples as the critical factor for prediction accuracy. (Franke K et al., 2007)

Another study by Kim DM, et al. they studied MR signal intensity of gray matter/white matter contrast and intracranial fat: effects of age and sex. On their study signal intensity (SI) values of gray- and white-matter brain (ROIs) were obtained from T(2)- and proton density-weighted magnetic resonance (MR) images of 58 normal subjects aged 22-82 years (31 females, 52.3+/-18.8 years; 27 males, 54.1+/-18.1 years). Sampled ROIs included the caudate, putamen, thalamus, orbitofrontal gyrus, gyrus rectus, uncus, frontal white matter, anterior and posterior corpus callosum, cranial-cervical junction fat, and retroorbital fat. Effects of age and sex on SI were examined using repeated-measures analysis of covariance. For both T(2)- and proton density-weighted acquisitions, a significant inverse relationship between age and SI was observed for the ratio of all summed gray-matter ROIs divided by summed white-matter ROIs. This relationship was additionally observed for ratios of both subcortical gray/white matter and cortical gray/white matter. Females compared with males had significantly lower cortical gray/white matter ratios on T(2)-weighted scans. Differences in SI were observed between cranial-cervical junction fat and retroorbital fat on both acquisitions, with females showing significantly higher values for cranial-cervical junction fat and males showing higher values for retroorbital fat. (Kim DM et al., 2002).

And DH Salat et al., also studied Age-Associated Alterations in Cortical Gray and White Matter Signal Intensity and Gray to White Matter Contrast

cortical surface models of 148 individuals was created and mapped regional gray and white matter T1-weighted signal intensities from 3D MPR images to examine patterns of age-associated signal alterations.

They found that gray matter intensity decreased with aging with strongest effects in medial frontal, anterior cingulate, and inferior temporal regions. White matter signal intensity decreased with aging in superior and medial frontal, cingulum, and medial and lateral temporal regions. The gray/white ratio was altered throughout a large portion of the cortical mantle, with strong changes in superior and inferior frontal, lateral parietal, and superior temporal and precuneus regions demonstrating decreased overall contrast. Statistical effects of contrast changes were stronger than those of cortical thinning. That results demonstrate that there are strong regional changes in neural tissue properties with aging and tissue intensity measures may serve as an important biomarker of degeneration. Their Study was result in:

Gray and white matter intensity showed regional decreases with age. Gray matter effects were found in medial frontal and anterior cingulate and lateral and inferior temporal regions with smaller effects apparent in frontal cortex. White matter signal decreases were strongest in superior and medial frontal and anterior cingulum regions with lesser effects in inferior temporal regions. The overlap in gray and white matter signal changes was regionally specific, and the age effects in white matter signal were to a greater spatial extent than gray matter. The gray white ratio significantly increased with age towards a value of 1 in a large portion of frontal regions, as well as inferior parietal, superior temporal, precuneus, and retrosplenial regions demonstrating a reduction in the contrast of these regions the authors next performed a similar analysis looking at the effects of age on regional white matter intensity regressing out gray matter

intensity at the adjacent cortical point on the surface. Results of this analysis were similar to the gray white ratio analysis; however the statistical effect was stronger when they performed the analysis with this statistical control DH. (Salat et al., 2010).

Also Ge Y Grossman et al. studied the effects of age and sex on total fractional GM (%GM) and total fractional WM (%WM). volumes was investigated by using volumetric MR imaging in healthy adults. Fifty-four healthy volunteers (22 men, 32 women) aged 20-86 years underwent dual-echo fast spin-echo MR imaging. Total GM, total WM, and intracranial space volumes were segmented by using MR image-based computerized semi automated software. Volumes were normalized as a percentage of intracranial volume (%GM and %WM) to adjust for variations in head size. Age and sex effects were then assessed. Their study showed both %GM and %WM in the intracranial space were significantly less in older subjects ($> \text{ or } = 50$ years) than in younger subjects (< 50 years), %GM decreased linearly with age, beginning in the youngest subjects. %WM decreased in a quadratic fashion, with a greater rate beginning only in adult midlife. Although larger GM volumes were observed in men before adjustments for cranium size, no significant differences in %GM or %WM were observed between the sexes. (Ge Y Grossman et al., 2002)

Chapter three

Materials and methods

3-1 materials:

3-1-1 location of the study:

This is a descriptive analytical study. It was conducted in Khartoum- Sudan, Garash International Specialized Hospital, during the period from June up to November 2014

3-1-2 Inclusion and exclusion criteria:

Sixty normal subjects (25 were males, 35 were females) with different ages (ranges between 14-70 years old) were selected consecutively on this study. All the selected patients were of normal MRI diagnosis, reported by experienced Radiologist .The reports showed No changes either in the brain size or texture. Patients with hypertension, diabetes, or lesion affected the brain signal intensity were excluded.

3-1-4 Instrumentation:

MRI 1.5 Tesla Toshiba Vantage was used on this study. Neurovascular coil was chosen

3-2 Methods:

3-2-1 Examination technique:

After optimizing all the safety requirements for the subjects to introduced to the MRI room and after full instructions about the nature of the examination ;the subjects lied in supine position on the MRI couch ,with the head first and then

the head localized on the neurovascular coil considering the longitudinal centering laser light overlapped with the medial sagittal plane and the transverse one localized at the nasion.

Three scouts were taken as planning localizer and then axial T1 were planed at the area of the basal ganglia using TR=464, TE=12, slice thickness =5mm, Slices gap =1.5mm matrix size 192x 400. The resultant images were saved for the measurements.

3-2-2 Data collection:

Six regions were selected, three from gray matter (the head of caudate nucleus, the thalamus and the putamen) and three from the white matter; (the genu of corpus callosum, the forcipes minor and the corona radiata) were selected for each subject and then the signal intensity was measured for each ROI by drawing 4 x 2 mm sampling field on each one to find out the mean of the SI for every ROI and then the measurements were noted on the data collection sheet as the following:

While G1 stands for the signal intensity of the head of caudate nucleolus, G2 stands for the signal intensity of the thalamus, G3 stands for the signal intensity of the putamen. W1 stands for the signal intensity of the genu of the corpus callosum, W2 stand for the signal intensity of the forcipes minor and W3 stands for the signal intensity of the corona radiata

3-2-3 Data analysis:

Microsoft Excel and SPSS program version 16 were used to analyze the data of this study. T- Test was used to examine the correlation between the variables, the correlation is significant at p value <0.01.

Chapter Four

Results

Table 4.1 the patient classification according to gender

Gender	Frequency	Percentages%
Male	25	41.7%
Female	35	58.3%
Total	60	100%

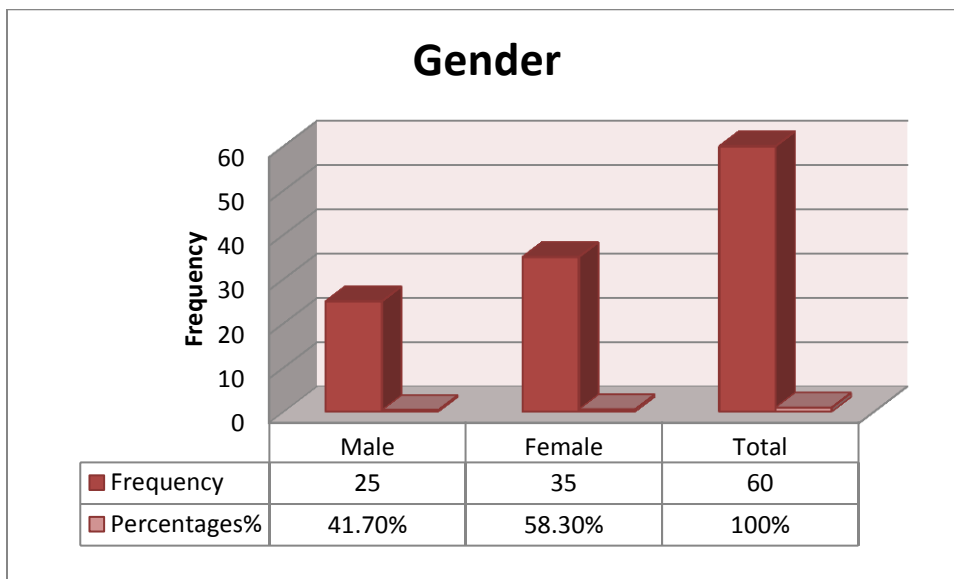


Figure4.1 The gender frequency and percentages

Table 4.2 the sample classification according to age classes

Age Classes	Frequency	Percentage%
14-28	30	50.0%
29-43	23	38.4%
44-58	5	8.3%
59-73	2	3.3%
Total	60	100%

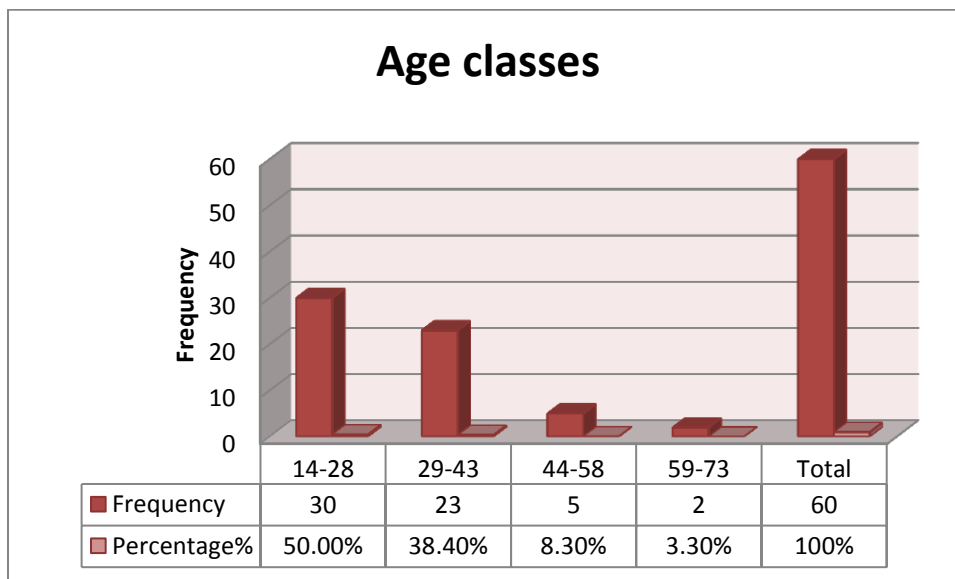


Figure 4.2 age classes, frequency and percentages

Table 4.3 *The descriptive statistics of the variables (Grey matter intensity, White matter intensity and age) mean, STDV, maximum and minimum values.*

Descriptive Statistics					
	N	Minimum	Maximum	Mean	Std. Deviation
G1	60	2197.00	3710.00	2.82	±413.17
G2	60	2205.00	3718.00	2.91	±422.55
G3	60	2310.00	5365.00	2.96	±511.86
W1	60	2450.00	4080.00	3.14	±428.86
W2	60	2650.00	4100.00	3.04	±555.76
W3	60	2384.00	4006.00	3.08	±435.27
Age	60	14.00	70.00	30.98	±11.84

G1 stands for GM at the head of the caudate nucleus, G2 stands for GM at the thalamus, G3 stands for GM at the putamen, W1 stands for WM at genu of corpus callosum, W2 stands for WM at the forcipes minor, W3 stands for WM at the corona radiata

		Correlations							
		G1	G2	G3	W1	W2	W3	Gender	Age
G1	Pearson	1	.991**	.650**	.967**	.653**	.914**	.017	-.737**
	Correlation								
G2	Sig. (2-tailed)		.000	.000	.000	.000	.000	.900	.000
	Pearson	.991**	1	.641**	.967**	.654**	.925**	.023	-.699**
G3	Correlation								
	Sig. (2-tailed)	.000		.000	.000	.000	.000	.859	.000
W1	Pearson	.650**	.641**	1	.614**	.406**	.583**	.085	-.469**
	Correlation								
W2	Sig. (2-tailed)	.000	.000		.000	.001	.000	.519	.000
	Pearson	.967**	.967**	.614**	1	.690**	.966**	.019	-.700**
W3	Correlation								
	Sig. (2-tailed)	.000	.000	.001	.000		.000	.594	.001
Gender	Pearson	.653**	.654**	.406**	.690**	1	.694**	-.070-	-.427**
	Correlation								
Age	Sig. (2-tailed)	.000	.000	.001	.000		.000	.594	.001
	Pearson	.914**	.925**	.583**	.966**	.694**	1	-.027-	-.581**
N	Correlation								
	Sig. (2-tailed)	.000	.000	.000	.000	.000		.839	.000
N	Pearson	.017	.023	.085	.019	-.070-	-.027-	1	-.119-
	Correlation								
N	Sig. (2-tailed)	.900	.859	.519	.887	.594	.839		.364
	Pearson	-	-	-	-.700**	-.427**	-	-.119-	1
N	Correlation								
	Sig. (2-tailed)	.737**	.699**	.469**			.581**		
N	N	60	60	60	60	60	60	60	60

** . Correlation is significant at the 0.01 level (2-tailed).

Table 4.4 the Correlations between the variables (2 tail test) G1 stands for GM at the head of caudate nucleus, G2 stands for GM at thalamus, G3 stands for GM at the putamen, W1 stands for WM at genu of corpus callosum, W2 stands for WM at the forcipes minor, W3 stands for WM at the corona radiata

Table 4.5 The coefficient of variable (G1) with age, Significance, R, R²

Coefficients						
	Unstandardized Coefficients		Standardized Coefficients	t	Sig.	R Square
	B	Std. Error	Beta			
Age	-25.721	3.093	-.737	-8.317	.000	.737
(Constant)	3626.130	102.479		35.384	.000	

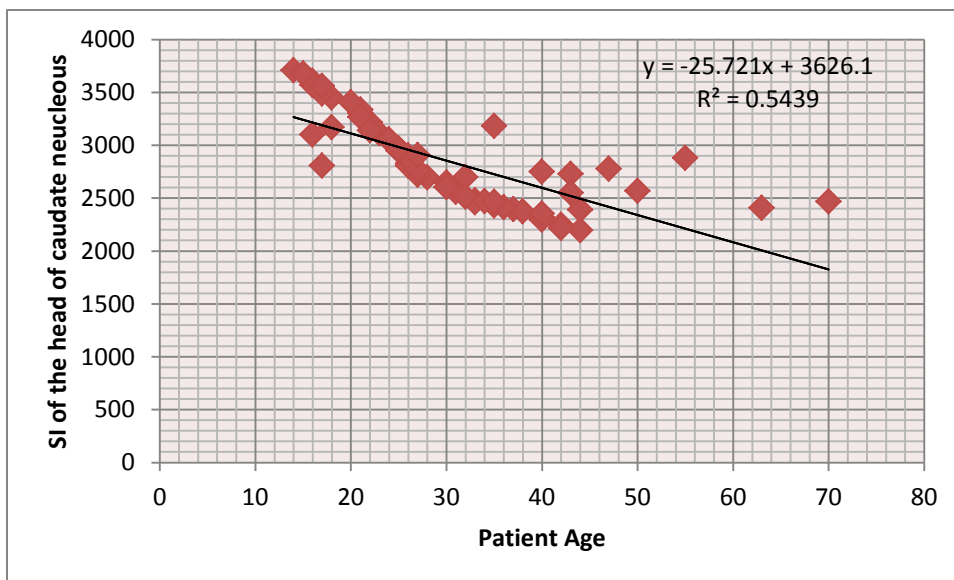


Figure4.3 Scatter plot shows the linear relationship between the age and the SI of the head of caudate nucleus (G1)

$$y = -25.72X + 3626$$

$$SI \text{ of the head of caudate nucleus} = -25.72(\text{age of new patient}) + 3626$$

$$Age = (SI \text{ of the head of caudate nucleus} - 3626) / -25.72$$

Table 4.6 The coefficient of variable (G2) with age, Significance, R, R²

Coefficients							
	Unstandardized Coefficients		Standardized Coefficients	t	Sig.	R	R Square
	B	Std. Error	Beta				
Age	-24.941-	3.348	-.699-	7.450-	.000	.699	.489
(Constant)	3686.29	110.933		33.230	.000		

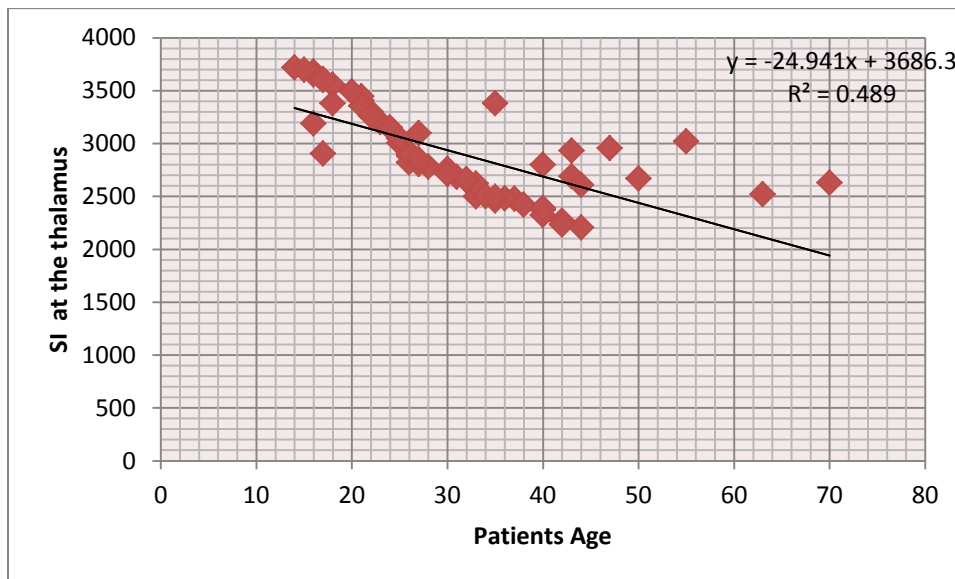


Figure4.4 Scatter plot shows the linear relationship between the age and the SI of the thalamus G 2

The relationship is made up by the following equation:

The signal intensity of the thalamus = $-24.94 \times \text{age of the normal object} + 3686$

So the age of the normal subject = (the SI of the thalamus - 3638) / -24.94

Table 4.7 the coefficient of variable (G3) with age, Significance, R, R²

Coefficients						
	Unstandardized Coefficients		Standardized Coefficients	t	Sig.	R
	B	Std. Error	Beta			
Age	-20.245	5.012	-.469	-4.040	.000	.469
(Constant)	3589.520	166.070		21.614	.000	

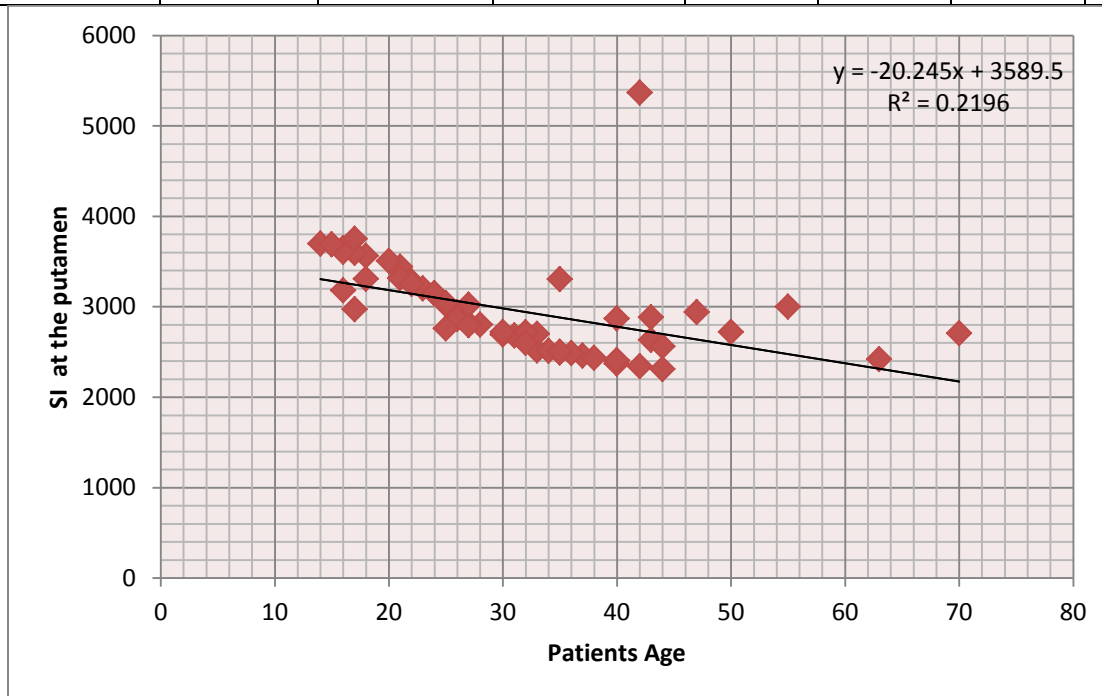


Figure4.5 Scatter plot shows the linear relationship between the age and putamen G 3

the intensity of the putamen decreases by 20.24 starting from 3589 /year,
 $r^2=0.219$

The SI of the putamen = $-20.24 \times \text{age of the normal object} + 3589$

the age of normal object = $(\text{SI of the putamen}-3589)/-20.24$

Table 4.8 The coefficient of variable (W1) with age, Significance, R, R²

Coefficients						
	Unstandardized Coefficients		Standardized Coefficients	t	Sig.	R
	B	Std. Error	Beta			R Square
Age	-25.329	3.396	-.700	-7.459	.000	.700
(Constant)	3927.88	112.526		34.906	.000	

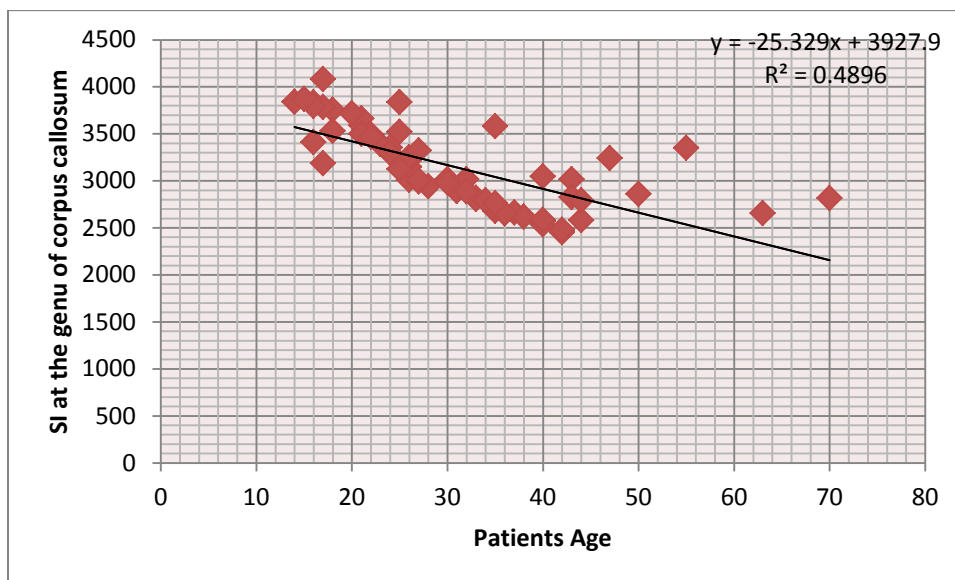


Figure 4.6 Scatter plot shows the linear relationship between the age and genu of corpus callosum W1

, the intensity of the genu of corpus callosum decreases by 25.32 starting from 3927 /year, $r^2=0.489$

The SI of the genu of corpus callosum = $-25.32 \times \text{age} + 3927$

the age = $(\text{SI of the genu of corpus callosum} - 3927) / -25.32$

Table 4.9 The coefficient of variable (W2) with age, Significance, R, R²

Coefficients							
	Unstandardized Coefficients		Standardize d Coefficients	t	Sig.	R	R Square
	B	Std. Error	Beta				
Age	-20.032-	5.570	-.427-	-3.596-	.001	.427	.182
(Constant)	3666.648	184.564		19.867	.000		

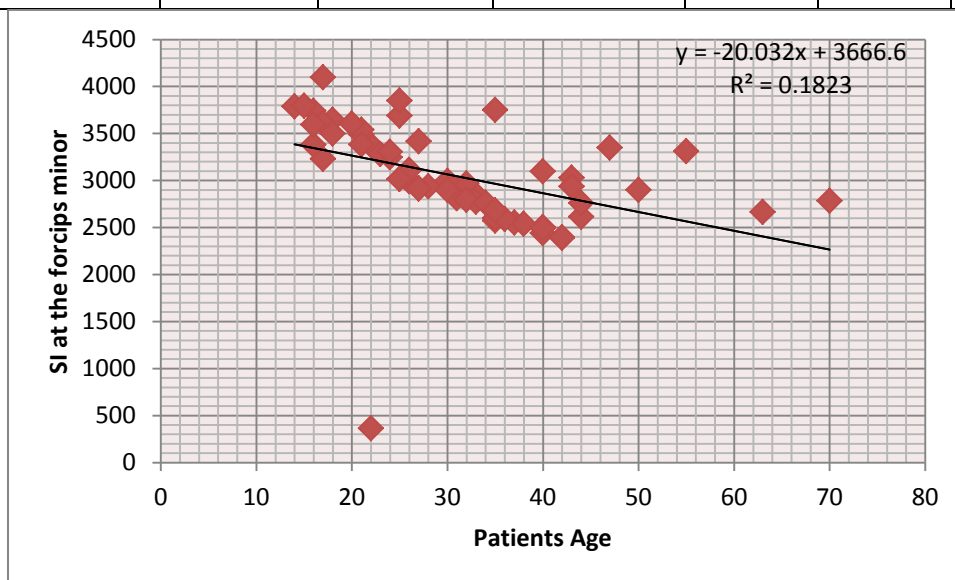


Figure4.7 Scatter plot shows the linear relationship between the age and forcipes minor W 2

The SI of the forcipes minor = (-20.03 x age) + 3666

$$\text{the age} = (\text{SI of the forcipes minor} - 3666) / -20.03$$

Table 4.10 The coefficient of variable (W3) with age, Significance, R, R^2

Coefficients							
	Unstandardized Coefficients		Standardized Coefficients	T	Sig.		
	B	Std. Error	Beta			R	R Square
Age	-21.336	3.928	-.581	-5.433	.000	.581	.337
(Constant)	3750.976	130.141		28.822	.000		

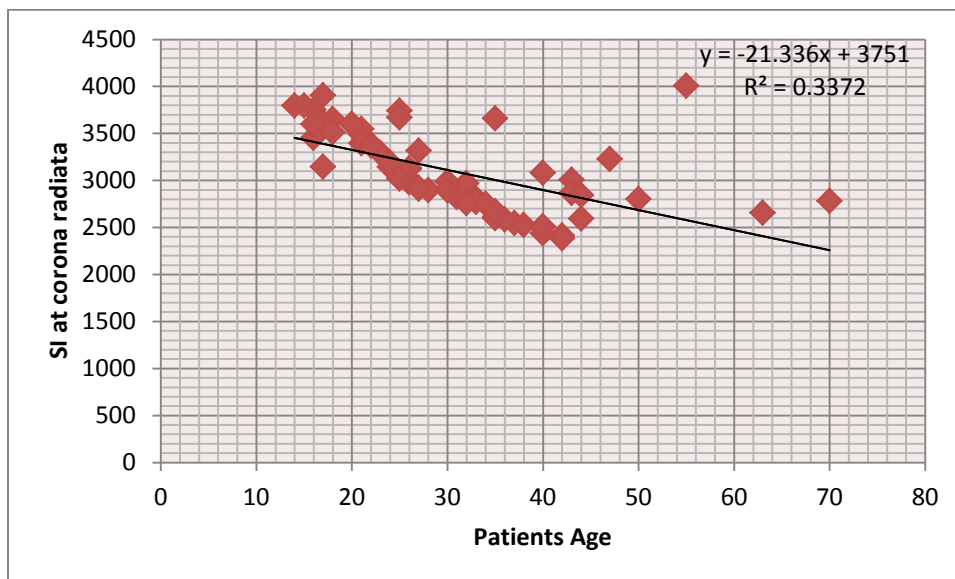


Figure 4.8 Scatter plot shows the linear relationship between the age and corona radiata W3

The signal intensity of the corona radiata = $-21.33 \times \text{age} + 3751$

$$\text{the age} = (\text{SI of the corona radiata} - 3751) / -21.33$$

The following tables presented the impact of gender on the variables (Gray and white matter intensities).

Table 4.11 The coefficient of variable (G1) with Gender, Significance, R, R²

Coefficients							
	Unstandardized Coefficients		Standardized Coefficients	T	Sig.		
	B	Std. Error	Beta			R	R Square
Gender	13.743	109.109	.017	.126	.900	.017	.000
(Constant)	2807.457	180.937		15.516	.000		

Table 4.12 The coefficient of variable (G2) with Gender, Significance, R, R²

Coefficients							
	Unstandardized Coefficients		Standardized Coefficients	t	Sig.		
	B	Std. Error	Beta			R	R Square
Gender	19.840	111.569	.023	.178	.859	.023	.001
(Constant)	2882.120	185.017		15.578	.000		

Table 4.13 The coefficient of variable (G3) with Gender, Significance, R, R²

Coefficients							
	Unstandardized Coefficients		Standardized Coefficients	t	Sig.		
	B	Std. Error	Beta			R	R Square
Gender	87.309	134.702	.085	.648	.519	.085	.007
(Constant)	2824.011	223.377		12.642	.000		

Table 4.14 *The coefficient of variable (W1) with Gender, Significance, R, R²*

Coefficients							
	Unstandardized Coefficients		Standardized Coefficients	t	Sig.		
	B	Std. Error	Beta			R	R Square
Gender	16.217	113.247	.019	.143	.887	.019	.000
(Constant)	3117.423	187.800		16.600	.000		

Table 4.15 *The coefficient of variable (W2) with Gender, Significance, R, R²*

Coefficients							
	Unstandardized Coefficients		Standardized Coefficients	t	Sig.		
	B	Std. Error	Beta			R	R Square
Gender	-78.446-	146.421	-.070-	-.536-	.594	.070	.005
(Constant)	3170.206	242.811		13.056	.000		

Table 4.16 *The coefficient of variable (W3) with Gender, Significance, R, R²*

Coefficients							
	Unstandardized Coefficients		Standardized Coefficients	t	Sig.		
	B	Std. Error	Beta			R	R Square
Gender	-23.486-	114.920	-.027-	-.204-	.839	.027	.001
(Constant)	3127.086	190.573		16.409	.000		

Chapter five

Discussion, conclusion and recommendations

5.1. Discussion

This study aimed to estimate the human age by measuring the MRI signal intensity of the brain in normal subjects.

The data of this research were collected from sixty normal subjects in both genders and different age ranges from fourteen up to seventy years old. All subjects were scanned using MRI on Garash international specialized hospital; the data were collected directly from the scanner computer and noted on the data collection sheet. The duration of data collection was extending from June up to November 2014. The data were analyzed using Microsoft Excel and SPSS program, the result of analysis came out as the following:

the correlation between the variables shows significant negative relationship between the MR signal intensity of the head of caudate nucleus and the age of the normal subjects ($R = -.737$). The relationship between signal intensity of the thalamus and age was found to be significant ($R = -.699$) also the signal intensity of the putamen showed significant relationship with age ($R = -.469$)

For white matter also the relationship between the MR signal intensity of the genu of corpus callosum and the subjects age is significant ($R = -.700$). The signal intensity of the forcipes minor also showed significant relationship with age ($R = -.427$) while the signal intensity of the corona radiata showed significant relationship with age ($R \text{ value} = -.581$)

the relationship between the age of normal subject and signal intensities of their ROIs and the equations that govern each relation were established for subjects with known ages as the following:

$$\text{Age of normal subject} = (SI \text{ of the head of caudate nucleus } -3626) / -25.72$$

$$= (SI \text{ of the thalamus} -3638) / -24.94$$

$$= (SI \text{ of the putamen} -3589) / -20.24$$

$$= (SI \text{ of the genu of corpus callosum } -3927) / -25.32$$

$$= (SI \text{ of the forcipes minor } - 3666) / -20.03$$

$$= (SI \text{ of the corona radiata } - 3751) / -21.33$$

On this study we found that the MRI signal intensity of both gray and white matter decay by aging process, this result agree with DH Salat 'et al.' study which result in that the gray and matter intensity decreased with aging.

But especially the MRI signal intensity of the head of caudate nucleus, thalamus, genu of corpus callosum and corona radiata shows very significant relationship with the subject's age.

5.2 Conclusion:

Beside diagnostic purposes and research MRI can also be used to estimate the human age by measuring the brain gray/white matter signal intensity for the normal subjects.

Signal intensity varies from subject to another due to normal aging. by excluding the NVD patients and any subject that may be affected by any other disorders that can affect the normal histology of brain we can find out how the

normal ageing affecting the brain tissue structure by measuring the MRI signal intensity of the brain tissue and correlate the result with the subjects age and then the equations that govern the relationship between those variables could easily be found out

5.3 Recommendations:

Further researches in wide field is recommended for this topic by increasing number of data, narrowing the exclusion criteria, and classification of the all affecting factors of brain MRI signal intensity

References:

Catherine and Carolyn (2000) MRI in practice. Second edition. London: Blackwell

DH. Salat et al., (2010). Age-Associated Alterations in Cortical Gray And White Matter Signal Intensity and Gray to White Matter Contrast {WWW} Available From
[Http://Www.Ncbi.Nlm.Nih.Gov/Pubmed/?Term=Rosas%20H%5Bauth%5D](http://Www.Ncbi.Nlm.Nih.Gov/Pubmed/?Term=Rosas%20H%5Bauth%5D). 5.1.2015

Franke K et al. (2007).Estimating The Age of Healthy Subjects from T1-Weighted MRI Scans Using Kernel Methods. University Of Jena, Jena, Germany {WWW} Available From
[Http://Www.Ncbi.Nlm.Nih.Gov/Pubmed/20070949](http://Www.Ncbi.Nlm.Nih.Gov/Pubmed/20070949). 25.1.2015

Ge Y Grossman 'Et Al.' 2002 Age-Related Total Gray Matter And White Matter Changes In Normal Adult Brain. Part I: Volumetric MR Imaging Analysis {WWW} Available From
[Http://Www.Ncbi.Nlm.Nih.Gov/Pubmed/12223373#](http://Www.Ncbi.Nlm.Nih.Gov/Pubmed/12223373#) 26/6/2014

Gilmore JH, Et Al.; 2006. 3 Tesla Magnetic Resonance Imaging of the Brain in Newborns. psychiatry research. 132(1):81–85.

Kanar Alkass et al., (2009) Age Estimation in Forensic Sciences

Kar-Ming Fung (2006) Neuropathology Lecture Note

Kim DM, 'Et Al.' (2002). MR Signal Intensity of Gray Matter/White Matter Contrast and Intracranial Fat: Effects of Age and Sex. {Www} Available From
[Http://Www.Ncbi.Nlm.Nih.Gov/Pmc/Articles/PMC25854](http://Www.Ncbi.Nlm.Nih.Gov/Pmc/Articles/PMC25854) 20/6/12/2014

M.A. Brown and R.C.Semelka 2003. C. MRI: Basic Principles & Applications. 3rd Ed. New Jersey. John Wiley & Sons, Inc., Hoboken
Maria and Leslie (2006) a Text Book Of Neuroanatomy London:
Blackwell

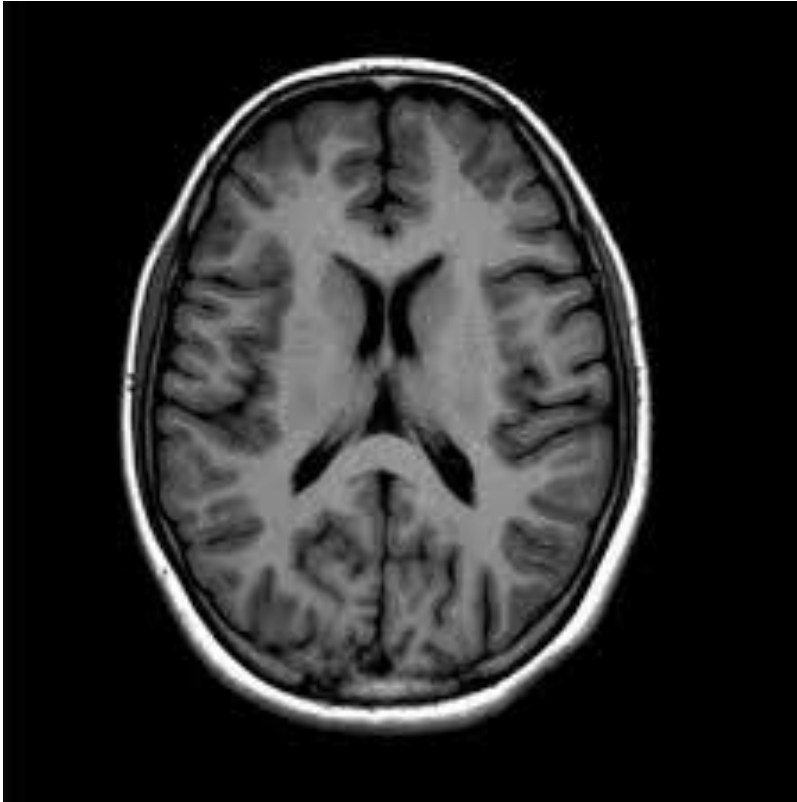
Valerie C. Scanlon (2007) Essentials of Anatomy and Physiology. Fifth
Edition – Philadelphia: F.A.Davis Company

Wallaby 2011. Which Factors Can Influence The Signal Intensity In
[MRI?](#){Www}.Available From

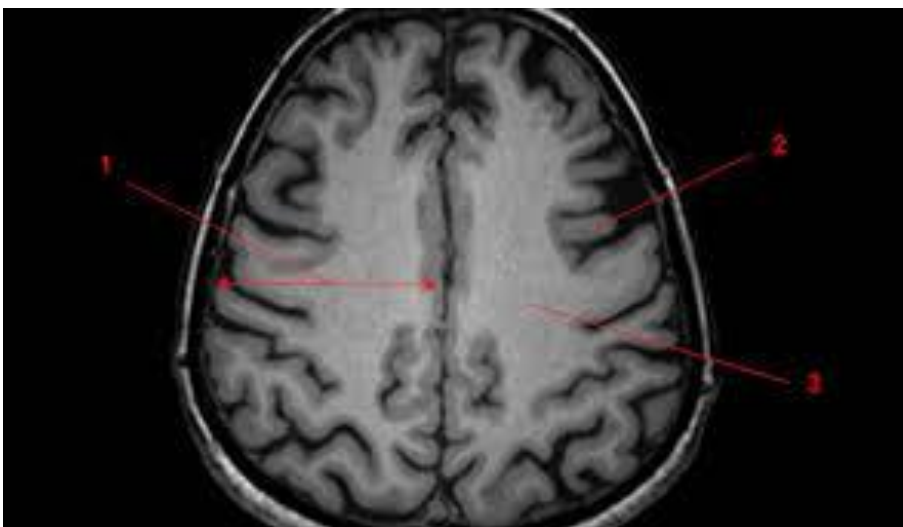
[Http://Www.Thescienceforum.Com/Physics/25012-Factors-Can-Influence-Signal-Intensity-Mri.Html](http://Www.Thescienceforum.Com/Physics/25012-Factors-Can-Influence-Signal-Intensity-Mri.Html) 28/10/2014

Wiki books Contributors (2007) Human Physiology

appendices



Normal MRI T1. section at the region of the basal ganglia for 42 years old male



MRI T1 section at the region of the corona radiata (pointed number 3)